Chinese Journal of Natural Medicines

Wenxia Changfu Formula inhibits NSCLC metastasis by halting TAMs-induced epithelial-mesenchymal transition *via* antagonisticallymodulating CCL18

Qianyu Bi, Mengran Wang, Li Luo, Beiying Zhang, Siyuan Lv, Zengna Wang, Xuming Ji

Citation: Qianyu Bi, Mengran Wang, Li Luo, Beiying Zhang, Siyuan Lv, Zengna Wang, Xuming Ji, Wenxia Changfu Formula inhibits NSCLC metastasis by halting TAMs-induced epithelial-mesenchymal transition *via* antagonisticallymodulating CCL18, Chinese Journal of Natural Medicines, 2025, 23(7), 838-847. doi: 10.1016/S1875-5364(25)60912-5.

View online: https://doi.org/10.1016/S1875-5364(25)60912-5

Chinese Journal of Natural Medicines 23 (2025) 838-847

Contents lists available at ScienceDirect

Chinese Journal of Natural Medicines

journal homepage: www.cjnmcpu.com/

Original article

Wenxia Changfu Formula inhibits NSCLC metastasis by halting TAMs-induced epithelial-mesenchymal transition *via* antagonistically modulating CCL18

Qianyu Bi[a,Δ], Mengran Wang[b,Δ], Li Luo[a,Δ], Beiying Zhang[c], Siyuan Lv[a], Zengna Wang[a], Xuming Ji[a,*]

[a] *School of Basic Medical Sciences, Zhejiang Chinese Medical University, Hangzhou 310000, China*
[b] *Department of Pediatrics, Affiliated Hospital of Shandong University of Traditional Chinese Medicine, Jinan 250000, China*
[c] *Taizhou Enze Medical Center (Group) Enze Hospital, Taizhou 318000, China*

ARTICLE INFO

Article history:
Received 12 August 2024
Revised 18 October 2024
Accepted 24 December 2024
Available online 20 July 2025

Keywords:
Tumor-associated macrophages
Non-small cell lung cancer (NSCLC)
Wenxia Changfu Formula
Chemokine (C-C motif) ligand 18 (pulmonary and activation-regulated) (CCL18)
Tyrosine-protein kinase Src

ABSTRACT

Our previous research demonstrated that the Wenxia Changfu Formula (WCF), as a neoadjuvant therapy, inhibits M2 macrophage infiltration in the tumor microenvironment and prevents lung cancer metastasis. Given tumor-associated macrophages (TAMs) in epithelial-mesenchymal transition (EMT), this study investigated whether WCF impedes lung cancer metastasis by attenuating TAM-induced EMT in non-small cell lung cancer (NSCLC) cells. Utilizing a co-culture model treated with or without WCF, we observed that WCF downregulated cluster of differentiation 163 (CD163) expression in macrophages, reduced CCL18 levels in the conditioned medium, and inhibited the growth, invasion, and EMT of NSCLC cells induced by macrophage co-culture. Manipulation of CCL18 levels and Src overexpression in NSCLC cells revealed that WCF's effects are mediated through CCL18 and Src signaling. *In vivo*, WCF inhibited recombinant CCL18 (rCCL18)-induced tumor metastasis in nude mice by blocking Src signaling. These findings indicate that WCF inhibits NSCLC metastasis by impeding TAM-induced EMT *via* antagonistic modulation of CCL18, providing evidence for its potential development and clinical application in NSCLC patients.

1. Introduction

Non-small cell lung cancer (NSCLC) remains one of the most prevalent malignancies worldwide [1]. Despite progressive improvements in therapeutics, the prognosis for NSCLC patients remains poor, with 5-year survival rates consistently low [2]. Recurrence and metastasis are primary factors contributing to treatment failure in NSCLC patients. Epithelial-mesenchymal transition (EMT) plays a crucial role in the metastasis cascade of NSCLC. EMT-tumor cells create an advantageous environment for their growth by modulating stromal cells. The tumor microenvironment comprises heterogeneous cell types, including infiltrating immune cells, endothelial cells, cancer-associated fibroblasts, extracellular matrix, and other stromal components. Among these, tumor-associated macrophages (TAMs) are major components of stromal cells and secrete various cytokines that regulate tumor growth and metastasis. Clinical and experimental evidence demonstrates that the interaction between the role of TAMs and cancer cells is involved in the occurrence, recurrence, and metastasis of NSCLC [3, 4]. Given the significance of TAMs in cancer metastasis, the mechanisms underlying the communication between TAMs and cancer cells have garnered considerable attention in research. For instance, CCL18 triggers are associated with cell stemness, NSCLC tumorigenesis, metastasis, and multidrug resistance [5]. TAM-derived CCL18 is essential for metastasis through the activation of Src/extracellular signal-regulated kinase (ERK)1/2 signaling. Studies have shown that Src/ERK1/2 activation is related to the interaction between cancer cells and the tumor microenvironment, which apparently promotes the EMT of cancer cells [6, 7]. Additionally, research has confirmed that THP-1 macrophages co-cultured with cancer cells exhibit characteristics of TAMs [8, 9]. In this study, NSCLC cells were co-cultured with THP-1 macrophages to establish an experimental system for investigating the malignant phenotype of NSCLC cells, macrophage polarization, and potential mechanisms.

Wenxia Changfu Formula (WCF) is a traditional Chinese medicine (TCM) formula comprising Aconiti Lateralis Radix Praeparata, Ginseng Radix et Rhizoma, Angelicae Sinensis Radix, and Radix et Rhizoma Rhei. *In vitro* and *in vivo* analyses have demonstrated that WCF is a potent anti-carcinogenic agent that inhibits multiple signaling pathways, inducing apoptosis and cell cycle arrest [10]. Our previous studies revealed that WCF could regulate the JAK3/signal transducer and activator of transcription 6 (STAT6)/PPARγ signal pathway and reduce M2 macrophage infiltration of tumor tissue. Notably, research has shown that WCF extract could inhibit migration and invasion of A549 cells in subcutaneous transplantation in nude mice by suppressing matrix metalloproteinase 2 (MMP2) and MMP9 [11]. Additionally, aconitine [12], emodin [13], and ginsenoside Rh2 [14], the active ingredients in WCF, modulated the crosstalk between TAMs and cancer cells

* Corresponding author.
E-mail address: jixuming724@163.com
Δ These authors contributed equally to this work.

https://doi.org/10.1016/S1875-5364(25)60912-5

and suppressed cancer metastasis. While experimental studies have provided a pharmacological basis for treating NSCLC with WCF, its detailed mechanism remains to be fully elucidated. Consequently, this study aims to assess whether and how WCF inhibits the metastasis of cancer cells induced by the co-culturing of macrophages and NSCLC cells.

2. Materials and methods

2.1. Cell lines and cell culture

A549, THP-1, and H460 cell lines were obtained from the Cell Bank of Type Culture Collection of the Chinese Academy of Sciences (Shanghai, China). All cells were generated and cultured according to previously described methods [15]. To obtain differentiated macrophages, THP-1 cells were treated with 320 nmol·L^{-1} phorbol 12-myristate 13-acetate (PMA, Sigma, P1585) for 6 h at 37 °C.

2.2. WCF and WCF-contained serum preparation

The Chinese herbal medicine WCF was supplied by the Affiliated Hospital of Zhejiang Chinese Medical University (Supplementary Table S1). Aconiti Lateralis Radix Praeparata (12 g) and Ginseng Radix et Rhizoma (9 g) were soaked for 1 h, then decocted for 2 h. Subsequently, Angelicae Sinensis Radix (6 g) was added and decocted for 30 min, followed by Rhei Radix et Rhizoma (12 g), which was decocted twice for 15 min each. The resulting filtrates were concentrated to 2 g crude drug·mL^{-1} and stored at −20 °C. To obtain WCF-containing serum, rats were randomly assigned to either the WCF group or the control group. The WCF group received WCF (40 g·kg^{-1}) *via* gavage, while the control group received an equivalent volume of saline, administered twice daily for 3 d. Following a 12-h fast after the final gavage, rats were given one day's dosage of WCF. Blood was collected after 1 h, inactivated at 56 °C, and processed into freeze-dried powder as previously described [15].

2.3. Ultra performance liquid chromatography (UPLC)/quadrupole time-of-flight mass spectrometry (Q-TOF-MS) analysis of WCF

The standards and samples were separated using a gradient mobile phase comprising (A) acetonitrile and (B) 0.1% formic acid in water. Separation was achieved using a Thermo Hypersil GOLD column (100 mm × 2.1 mm, 1.9 μm, Boston, USA) maintained at 35 °C. The flow rate was set at 0.5 mL·min^{-1} with an injection volume of 1 μL. Mass spectrometry analysis was conducted on a Bruker Q-TOF instrument (Bruker, Germany) equipped with an electrospray ionization source (ESI) operating in positive ion mode. The electrospray source and desolvation temperatures were maintained at 200 and 325 °C, respectively. Nitrogen flow rate was established at 8 L·min^{-1}. The ESI capillary and cone voltages were set to 3500 and 30 V, respectively. For MS detection, accurate mass was maintained in full scan/data-dependent MS^2 (full MS/dd-MS^2) mode [16].

2.4. NSCLC-TAM co-culture model

To analyze the interactions between NSCLC cells and TAMs in the presence of WCF, co-culture models were established [17]. THP-1 macrophages were activated as previously described. Based on experimental requirements, THP-1 macrophages (5 × 10^3 per well in 24-well plate format or 1.2 × 10^4 per well in 6-well plate format) in a complete medium were plated in either the lower or upper chamber and cultured for 6 h. Subsequently, an equal number of tumor cells in complete medium were seeded in the opposite chamber and co-cultured for 48 h using a transwell system (pore diameter 0.4 μm, Corning Costar, NY, USA). Following this period, the THP-1 macrophage-activated tumor cells and the co-culture supernatant (Co-CM) were collected.

2.5. WCF treatment in vitro

To investigate the effects of WCF on co-cultures, THP-1 macrophages co-cultured with tumor cells were treated with or without WCF-containing serum for 48 h. Subsequently, the supernatant of co-culture (Co-CM + WCF) was collected. To determine the combined effects of CCL18 and WCF on A549 cell invasion induced by Co-CM, the tumor cells were treated with conditioned medium from Co-CM, either depleted of CCL18 by neutralizing antibody (AbCCL18, Bioss, China) or supplemented with recombinant CCL18 (rCCL18, Peprotech, USA), in the presence or absence of WCF (10%). To assess the relationship between Src activation in tumor cells and WCF treatment in co-cultured THP-1 macrophages with NSCLCs, the tumor cells expressing Src were treated with or without Co-CM in the presence or absence of WCF (10%).

2.6. Flow cytometry

To investigate the potential anti-tumor effects of WCF on NSCLC cells when co-cultured with TAMs, an apoptosis assay was conducted. Tumor cells were co-cultured with THP-1 macrophages in 6-well plates with WCF-containing serum (0, 7.5%, 10%, and 15%) for 48 h. Subsequently, cells were washed twice with phosphate-buffered saline (PBS), trypsinized, and collected by centrifugation at 1000 r·min^{-1} for 5 min. The cells were then resuspended to a concentration of 1 × 10^6 cells/mL, and apoptosis was assessed using an apoptosis kit (BD, NJ, USA) following the manufacturer's protocol. For macrophages, single-cell suspensions in PBS were stained with anti-human cluster of differentiation 163 (CD163) antibody (Proteintech, China) at 4 °C for 30 min. After three PBS washes, cells were analyzed using a CytoFlexs Beckman Coulter flow cytometer, and data were processed with CytExpert software.

2.7. Cell viability assay

Tumor cells (5 × 10^3 cells/well) were seeded into 24-well plates and co-cultured with THP-1 macrophages in the presence or absence of WCF-containing serum (0, 5%, 7.5%, 10%, 15%, 20%) for 48 h. Following incubation, cell viability was assessed using the CCK-8 assay as per the manufacturer's protocol. The optical density was measured at 450 nm using a microplate spectrophotometer (Tecan, M200 pro, Switzerland).

2.8. Wound healing assay

Cells (2 × 10^5 cells/well) were seeded into plates for 24 h, after which a cell-free line was created by manually scratching the confluent cell monolayers with a 200 μL pipette tip. The wounded cell monolayers were then washed with PBS and incubated in Roswell Park Memorial Institute (RPMI) 1640 medium containing WCF-supplemented serum for 24 h. Five scratched fields were randomly selected, and images were captured using a bright-field microscope (Nikon, Ts2, CHINA). The percentage of wound closure was subsequently quantified using ImageJ software.

2.9. Cell invasion assay

Cells (1 × 10^5 cells/well) were seeded in RPMI 1640 medium in the upper chamber of a transwell insert. The insert was precoated with BD Matrigel (BD, USA, 275001). A complete medium

(600 μL, containing 10% FBS) was added to the lower chamber. Following a 24-h incubation period, cells remaining on the upper surface of the membrane were gently removed. Migrated cells were fixed and subsequently stained with 0.5% crystal violet (Yuanye Biotech, Shanghai, China, 548-62-9). Cell quantification was performed using a bright-field microscope [11].

2.10. Ribonucleic acid (RNA) extraction and quantitative real-time polymerase chain reaction (qRT-PCR) assays

Total RNA was extracted from tissues or cultured cells using TRIzol reagent (Thermo Fisher) following the manufacturer's protocol. Subsequently, 1 μg RNA aliquots were reverse transcribed to cDNA in a final volume of 20 μL under standard conditions using an Evo M-MLV RT Premix for qPCR Kit (Accurate, Hunan, China). RT-PCR analyses were conducted using SYBR Green Premix Pro Taq HS qPCR Kit (Accurate, Hunan, China) on an Appliedbio system Quant Studio 3 Real-Time PCR System (ABI, USA). Gene expression was normalized to that of glyceraldehyde-3-phosphate de-hydrogenase (GAPDH) using the relative threshold cycle method and then converted to fold changes. The specific primers utilized are listed in Supplementary Table S2.

2.11. Enzyme-linked immunosorbent assay (ELISA)

Following WCF exposure, supernatants were collected from the lower chambers of 24-well plate format cell culture inserts. The release of interleukin (IL)-12, CCL18, and IL-10 was quantified using an ELISA kit according to the manufacturer's instructions (Multiscuences Biotech, Co., Ltd., Hangzhou, China).

2.12. Immunofluorescence assay

The cells were fixed with 4% paraformaldehyde and permeabilized using 0.25% Triton-X 100. Subsequently, an immunofluorescence assay was performed. Briefly, primary antibodies against *E*-cadherin, *N*-cadherin, and vimentin (Proteintech, Wuhan, China) were applied for overnight incubation at 4 °C, followed by staining with Cy3-conjugated secondary antibodies. After incubation with DAPI, images were captured using a fluorescent microscope (ZEISS Observer. A1, Germany).

2.13. Adenovirus infection

Transient overexpression of Src was accomplished through adenoviral infection using Ad-Src adenovirus for 72 h. The enhanced infection procedure was conducted according to the manufacturer's instructions (Jikai Gene Co., Ltd., Shanghai, China).

2.14. Western blot analysis

Protein extracts were probed using antibodies specific to Src (Cell Signaling Technology, China), phosphorylated (p)-Src (Cell Signaling Technology, China), ERK1/2 (Servicebio, Wuhan, China), p-ERK1/2 (Beyotime, Shanghai, China), *E*-cadherin (Proteintech, Wuhan, China), *N*-cadherin (Proteintech, Wuhan, China), and vimentin (Proteintech, Wuhan, China). A peroxidase-conjugated anti-rabbit antibody (Proteintech, Wuhan, China) served as the secondary antibody. The resulting blots were quantified *via* densitometry analysis using ImageJ software.

2.15. Systemic xenograft tumor model

BALB/c female nude mice (4–6 weeks old, weighing 16–20 g) were obtained from Shanghai SLAC Laboratory Animal Co., Ltd. (Shanghai, China). The animals were housed in groups of 4–5 per cage in a pathogen-free environment (55% ± 10% humidity, 22 ± 2 °C, and 12–12 h/light-dark cycle) with ad libitum access to standard laboratory water and diet. On day 0, mice received 2×10^6 luciferase-expressing A549 cells *via* tail vein (i.v.), followed by weekly bioluminescence imaging (BLI) monitoring. Upon confirmation of engraftment on day 8, the mice were randomized into four groups: i) the solvent control group; ii) the WCF group, receiving 20 g WCF·kg^{-1}·d^{-1} by gavage; iii) the rCCL18 group, receiving 0.1 μg·kg^{-1}·week^{-1} rCCL18 (i.v.); iv) the WCF + rCCL18 group, receiving 20 g WCF·kg^{-1}·d^{-1} by gavage + 0.1 μg·kg^{-1}·week^{-1} rCCL18 (i.v.). All mice were euthanized under excessive isoflurane (RWD, CHINA, R510-22-10) anesthesia when either experimental or humane endpoints were reached.

2.16. Bioluminescence imaging (BLI)

The IVIS Lumina XR III Imaging System with Living Image software 4.4 (PerkinElmer, USA) was utilized to acquire bioluminescence images. Mice were anesthetized and maintained under inhalational anesthesia using a nose cone with 2% isoflurane in medical oxygen. Prior to imaging, all mice received an intraperitoneal injection of 150 mg·kg^{-1} D-luciferin (Abcam, USA, Ab143655) in PBS. Imaging was conducted 10 min post-injection with a 12.5 cm field of view. Signal quantification was performed through region of interest analysis, with results expressed in radiance (unit of p·s^{-1}·cm^{-2}·sr^{-1}) as previously described [18].

2.17. Immunohistochemical staining

Previously prepared paraffin-fixed tissue sections underwent processing for peroxidase (DAB) immunohistochemistry. Following deparaffinization and rehydration using xylene and a series of decreasing ethanol concentrations (95%, 80%, 70%), 50 mL of 1∶500 diluted CCL18 primary antibody was applied to each sample. The samples were incubated overnight at 4 °C. After a 5-min water wash, the addition of peroxidase-labeled polymer and substrate facilitated the visualization of target proteins through brown staining. Subsequently, the samples were counterstained with hematoxylin for 30 sec.

2.18. Statistical analysis

Data were presented as mean ± standard error and analyzed using SPSS 26.0 software. Between-group comparisons were conducted using one-way analysis of variance (ANOVA). Statistical significance was established at $P < 0.05$.

3. Results

3.1. Chemical profiling of WCF

To analyze the chemical composition of WCF, UPLC/Q-TOF-MS was employed in both positive and negative-ion source modes (Supplementary Fig. S1). Twelve active components of WCF were identified using related standards and reported literature [19-22]. These components include salsolinol, aloesin, aloe-emodin, ferulic acid, senkyunolide H, emodin, ginsenoside Rb1, aconitine, ginsenoside Rg2, ginsenoside Rg3, genistein, and rubiadin. The detailed results are presented in the Supporting Table.

3.2. WCF reduced the effects of TAMs on the proliferation of NSCLC cells

Our findings demonstrated a significant increase in the proliferation capacity of NSCLC cells within the co-cultured system compared to isolated A549 and H460 cells. The addition of WCF resulted in decreased cell viability (Figs. 1A and 1B). Notably,

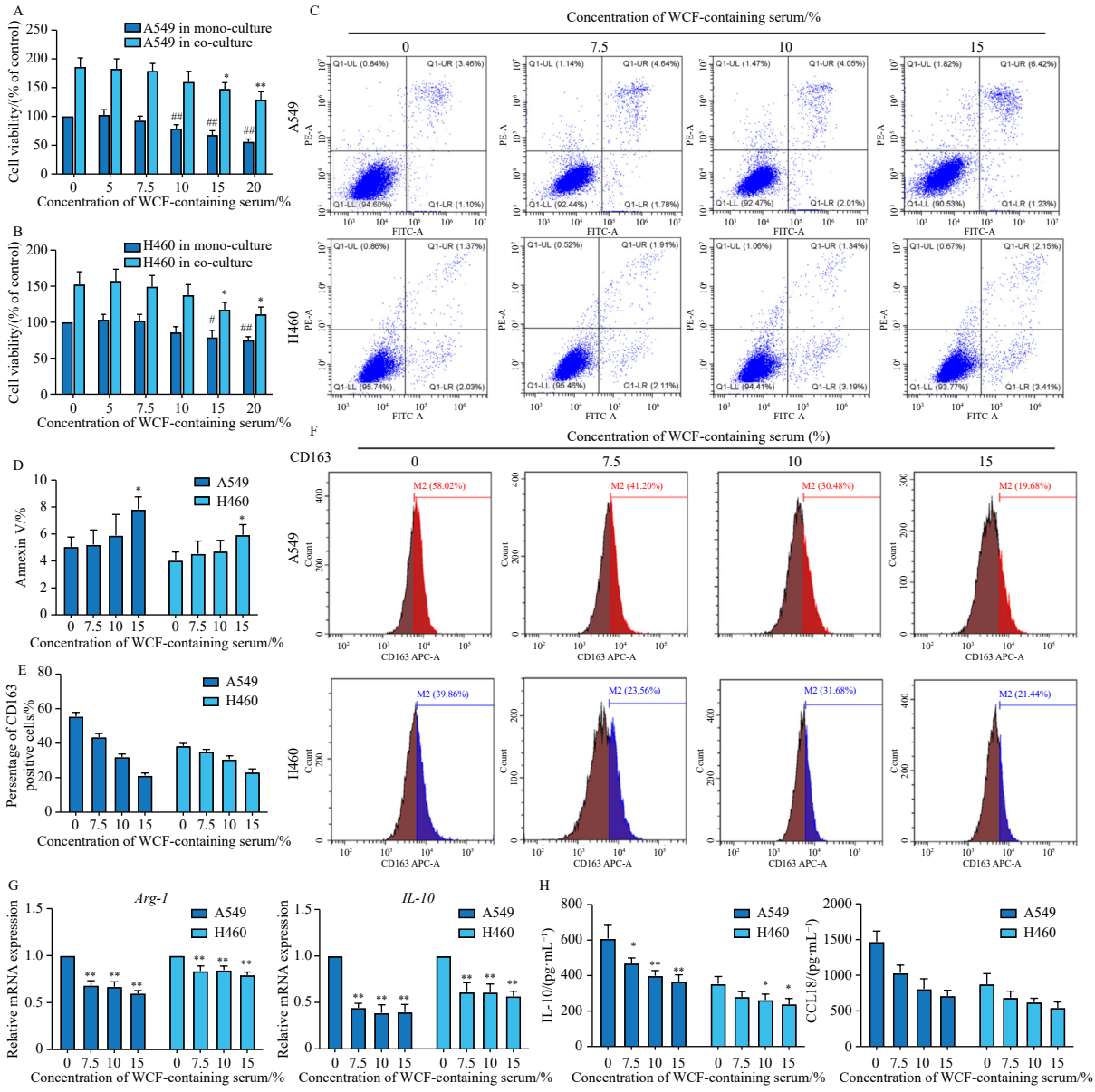

Fig. 1 WCF reduced the effects of TAMs on the proliferation of NSCLC cells. (A, B) Effects of WCF-containing serum exposure (0%–20%) after 48 h. (C, D) Annexin V/Propidium iodide (PI) staining was used to assess cell viability. (E, F) Flow cytometry was used to quantify the expression of CD163. (G) The levels of *Arg-1* and *IL-10* in the macrophages were measured by qRT-PCR. (H) The levels of IL-10 and CCL18 in the supernatant were measured by ELISA. Data are presented as the mean ± SD from three independent experiments. $^{*}P < 0.05$, $^{**}P < 0.01$ *vs* control. WCF, Wenxia Changfu Formula.

15% WCF-containing serum inhibited tumor cell viability, as evidenced by an increased proportion of Annexin V + tumor cells (Figs. 1C and 1D). Furthermore, in the co-cultured system, the percentage of CD163 + cells (a marker of M2-like TAMs) significantly decreased in the various WCF dosage groups compared to the control group (Figs. 1E and 1F). Gene expression analysis was conducted using qRT-PCR. *Arg-1* and *IL-10* were utilized as markers for M2 macrophages, while tumor necrosis factor-α (*TNF-α*), *IL-1β*, and inducible nitric oxide synthase (*iNOS*) served as markers for M1 macrophages. The results indicated reduced expression of *Arg-1* and *IL-10* in the WCF group compared to the control group (Fig. 1G). However, WCF exhibited minimal effect on the expression of *TNF-α*, *IL-1β*, and *iNOS* (Supplementary Fig. S2A). Additionally, WCF decreased the levels of IL-10 and CCL18 (Fig. 1H) in a dose-dependent manner without affecting IL-12 levels (Supplementary Fig. S2B) in Co-CM. These observations suggest that WCF may inhibit M2 polarization of THP-1 macrophages co-cultured with NSCLC cells.

3.3. WCF suppressed EMT of NSCLCs induced by Co-CM

Following treatment with or without WCF-containing serum, the Co-CM from the co-culture system of NSCLC cells/M2 macrophages was collected. Wound healing and transwell assays demonstrated that WCF suppressed the migration and invasive capacity of A549 and H460 cells induced by Co-CM (Figs. 2A–2D). Moreover, Co-CM containing WCF increased the protein expression level of the cancer cell EMT surface marker *E*-cadherin while decreasing the levels of *N*-cadherin and vimentin (Figs. 2E and 2F). These findings indicate that WCF could also inhibit the EMT of cancer cells induced by Co-CM.

3.4. Effects of CCL18 consumption or addition combined with WCF on A549 cell invasion induced by Co-CM

To assess the significance of CCL18 in TAM-mediated EMT in NSCLC cells, a CCL18-neutralizing antibody was introduced to the Co-CM. The findings revealed that the combined depletion of

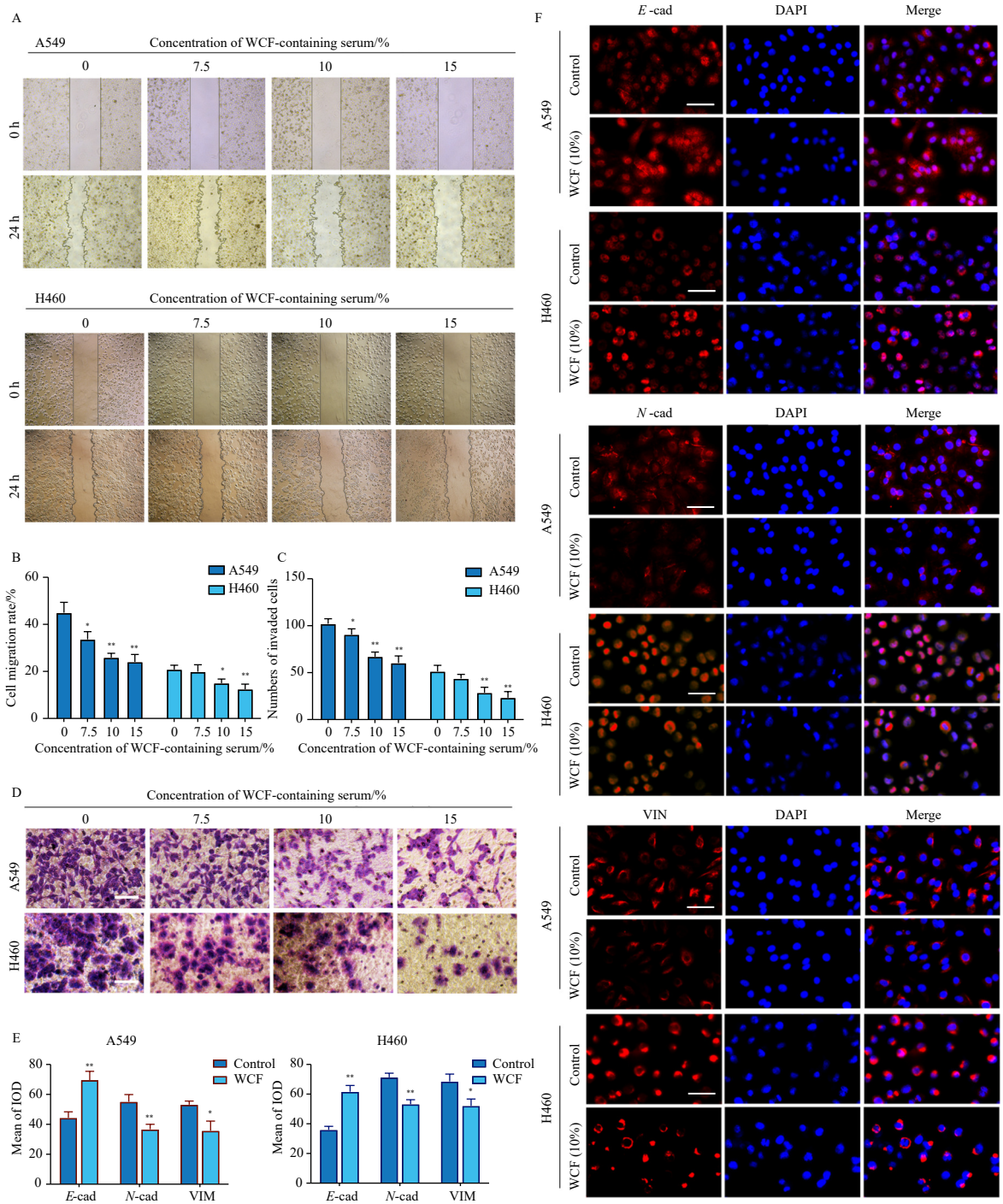

Fig. 2 WCF suppressed the M2-TAMs-induced EMT of NSCLC cells. (A–D) The migration and invasion were evaluated by wound healing assay and transwell assay, respectively (scale bar, 200 μm). (E, F) The expressions of EMT markers (*E*-cadherin, *N*-cadherin, and vimentin) were examined by immunofluorescence analysis (scale bars, 200 μm). Error bars represent mean values ± SD from three independent experiments. $^{*}P < 0.05$, $^{**}P < 0.01$ *vs* control. WCF, Wenxia Changfu Formula; *E*-cad, *E*-cadherin; *N*-cad, *N*-cadherin; VIM, vimentin.

CCL18 in Co-CM and WCF administration in the co-culture system diminished the invasive capacity of NSCLC cells (Figs. 3A and 3B). Additionally, this co-treatment elevated *E*-cadherin levels while reducing the phosphorylation of Src and ERK1/2, as well as the expression of *N*-cadherin and vimentin in NSCLC cells (Figs. 3C and 3D). Conversely, exogenous recombinant CCL18 significantly counteracted the WCF-induced increase in *E*-cadherin levels, decrease in Src and ERK1/2 phosphorylation, and reduction in *N*-cadherin and vimentin expression in A549 cells exposed to Co-CM (Figs. 3G and 3H). The introduction of recombinant CCL18 effectively reversed the Co-CM-induced suppression of NSCLC cell invasiveness mediated by WCF treatment (Figs. 3E and 3F). Furthermore, comparable results were observed in H460 cells (Supplementary Fig. S3).

3.5. Overexpression of Src enhanced invasion of A549 cells induced by Co-CM

To investigate the role of Src activation in WCF-mediated inhibition of NSCLC cell invasion, A549 cells expressing Src were utilized. This study demonstrated that Src overexpression enhanced A549 cell invasion (Figs. 4A and 4B). CCL18 blockade resulted in decreased invasion capabilities of A549 cells and reduced expression of p-SRC and p-ERK. The findings indicated that

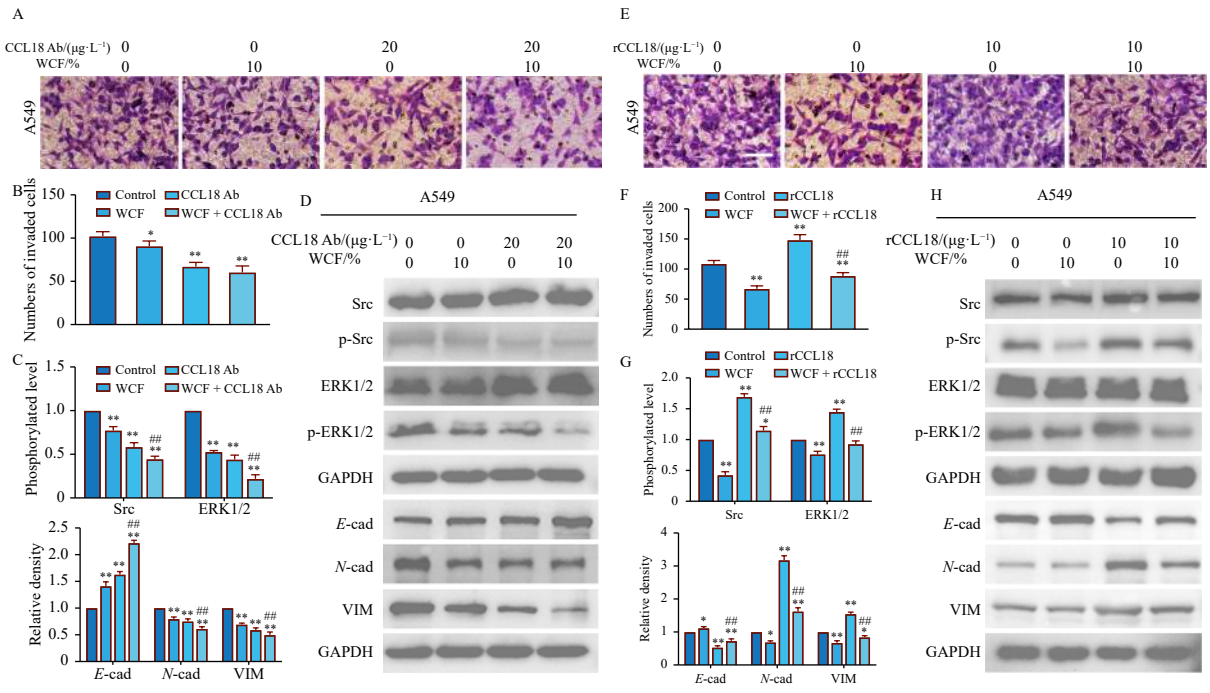

Fig. 3 Effects of CCL18 combined with WCF on the invasion of A549 cells induced by Co-CM. A549 cells were treated with conditioned medium (Co-CM) derived from THP-1-differentiated macrophages, with either depletion or supplementation of CCL18, in the presence or absence of WCF. (A, B) Transwell invasion assays were performed to assess the invasive capacity of A549 cells treated with CCL18-depleted Co-CM, WCF alone, or the combination of both (scale bar, 200 μm). (C, D) Western blotting analysis of A549 cells treated with WCF and CCL18 Ab for 24 h. (E, F) Transwell invasion assays evaluating the effects of recombinant CCL18 (rCCL18), WCF, or their combination on Co-CM-induced A549 cell invasion(scale bar, 200 μm). (G, H) Western blotting analysis of A549 cells treated with WCF and rCCL18 for 24 h. Data are presented as mean ± SD from three independent experiments. $^{*}P < 0.05$, $^{**}P < 0.01$ *vs* A549 cells treated with Co-CM; $^{\#}P < 0.05$, $^{\#\#}P < 0.01$ *vs* A549 cells treated with the conditioned medium obtained from WCF treatment. CCL18 Ab, CCL18 antibody; rCCL18, recombinant CCL18; *E*-cad, *E*-cadherin; *N*-cad, *N*-cadherin; VIM, vimentin.

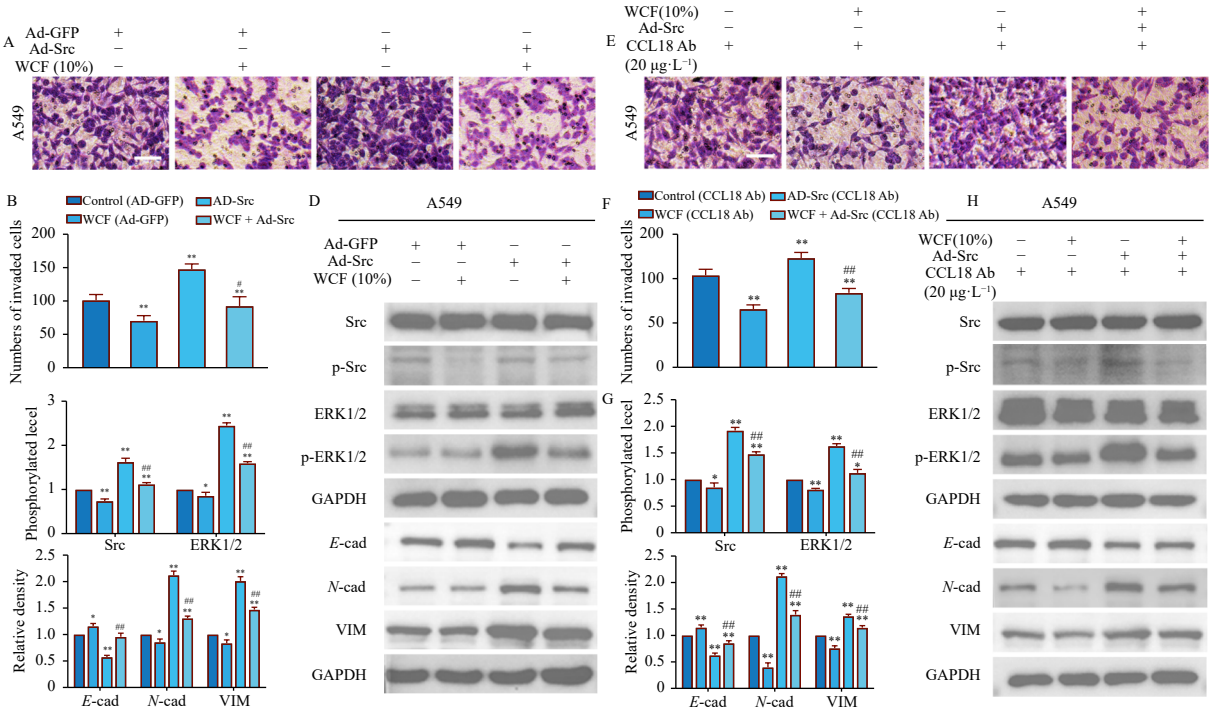

Fig. 4 Effects of Src on the invasion of A549 cells induced by Co-CM. A549 cells were treated with CCL18 depleting Co-CM from THP-1 macrophages co-cultured with A549 transduced with adenovirus expressing Src and in the presence or absence of WCF. Ad-Src: the cells transduced with adenovirus expressing Src. (A, B) The invasion of A549 cells induced by Co-CM in overexpression of Src and WCF alone or in combination were evaluated by transwell assay (scale bar, 200 μm). (C, D) Western blotting of A549 cells treated with WCF combined with Ad-Src for 24 h. $^{*}P < 0.05$, $^{**}P < 0.01$ *vs* Ad-GFP; $^{\#}P < 0.05$, $^{\#\#}P < 0.01$ *vs* Ad-GFP and WCF group. (E, F) The invasion of A549 cells induced by Co-CM were evaluated by transwell assay (scale bar, 200 μm). (G, H) Western blotting of A549 cells treated with WCF combined with Ad-Src and CCL18Ab for 24 h. $^{*}P < 0.05$, $^{**}P < 0.01$ *vs* depletion of CCL18; $^{\#}P < 0.05$, $^{\#\#}P < 0.01$ *vs* depletion of CCL18 and WCF. Error bars represent mean ± SD from three independent experiments. Ad-GFP, the cells transduced with adenovirus expressing GFP; Ad-Src, the cells transduced with adenovirus expressing Src; CCL18 Ab, CCL18 antibody; *E*-cad, *E*-cadherin; *N*-cad, *N*-cadherin; VIM, vimentin.

Src overexpression counteracted the effects of WCF, increasing *E*-cadherin expression while decreasing the phosphorylation levels of Src and ERK1/2, as well as the levels of *N*-cadherin and vimentin in A549 cells induced by Co-CM (Figs. 4C and 4D).

3.6. Src overexpression mitigated the combined effects of CCL18 depletion and WCF on NSCLC cell invasion

To elucidate the role of the CCL18-induced Src axis in WCF's inhibition of A549 cell invasion induced by Co-CM, we prepared Co-CM depleted of CCL18 for A549 cells expressing Src, with or without WCF treatment. Our findings demonstrated that Src overexpression diminished the inhibitory effect of CCL18 depletion combined with WCF on the invasive capacity of A549 cells induced by Co-CM (Figs. 4E and 4F). Moreover, Src overexpression counteracted the effects of CCL18 depletion combined with WCF, leading to increased *E*-cadherin levels and decreased *N*-cadherin and vimentin levels in A549 cells (Figs. 4G and 4H). Comparable results were observed in H460 cells (Supplementary Fig. S4).

3.7. WCF neutralized rCCL18 increased growth and metastasis of xenograft

The anti-tumor activity *in vivo* of WCF was evaluated using the NSCLC xenograft model (Fig. 5A). As anticipated, fluorescence intensity detected in mice and statistical analysis for *in vivo* metastasis assessment revealed that rCCL18 promoted tumor growth and metastasis *in vivo* compared to the control group, while WCF intervention mitigated these effects (Figs. 5B and 5C). Consistent findings were observed in H&E staining and statistical analysis of metastatic nodules in dissected lung specimens from mice (Figs. 5D and 5E). Immunohistochemistry testing demonstrated that CCL18 protein expression was downregulated in WCF-treated xenografts (Fig. 5F). Furthermore, immunofluorescence and Western blot assays showed significantly increased expression of EMT markers, p-Src, and p-ERK in rCCL18-treated xenografts (Figs. 5G–5I). Notably, *E*-cadherin expression was elevated, while *N*-cadherin and vimentin expression were reduced in the WCF + rCCL18 group compared to the rCCL18 group. Western blot analysis indicated that WCF neutralized rCCL18-induced activation of the Src/ERK1/2 signaling pathway (Fig. 5I). Collectively, these findings suggest that WCF neutralized rCCL18-enhanced growth and metastasis of xenografts.

4. Discussion

TAMs are recognized as the predominant inflammatory cells within the tumor microenvironment, playing a crucial role in various stages of lung cancer progression [23, 24]. Typically, TAMs in the tumor microenvironment primarily exhibit M2-like characteristics and secrete substantial quantities of chemokines that contribute to tumor development [25]. Among these chemokines, CCL18 stands out as one of the most significant secreted by TAMs [26]. Recent investigations have demonstrated that serum CCL18 levels are markedly elevated in patients with NSCLC, and these levels correlate with overall survival rates and tumor stages [27, 28].

Previous research has established WCF as a potent anti-carcinogenic agent, with findings suggesting that the chemokine signaling pathway might play a crucial role in its therapeutic mechanism. In the current study, our results demonstrated that WCF reduced the percentage of $CD163^+$ THP-1 macrophages and decreased the invasive ability of A549 cells in the co-culture system of NSCLC cells/THP-1 macrophages. Furthermore, WCF reduced the levels of IL-10 and CCL18 in Co-CM, indicating its ability to reverse the M2 polarization of THP-1 macrophages. Given that EMT plays a critical role in cell invasion and metastasis of tumors [29], we explored the effect of WCF treatment on the co-culture system and the expression of EMT markers in tumor cells. Our research revealed that WCF increased the protein expression of *E*-cadherin and decreased the levels of *N*-cadherin and vimentin in NSCLC cells induced by Co-CM. These results provide evidence that WCF disrupts the interaction between NSCLC cells and TAMs, inhibiting EMT of cancer cells induced by co-culture. Subsequently, we investigated the molecular mechanisms involved in WCF-induced tumor inhibition within this co-culture system.

CCL18 has been shown to activate several intracellular signaling pathways downstream of receptors such as the phosphatidylinositol transfer protein 3 (PITPNM3)/PYK2 *N*-terminal domain-interacting receptor 1 (Nir1) and CCR8 [30]. Research indicates that CCL18 triggers activation of Src signal transduction, which is associated with migration induction, invasion, and EMT of cancer [31, 32]. Src, a proto-oncogene, has been identified as having abnormal activation closely related to the development of various cancers, including lung cancer [33]. Oncogenic signal transduction is tightly regulated by Src and Src-mediated complex pathways, including ERK1/2, JNK, PI3K-AKT, and STAT3 [34, 35]. The Src/ERK1/2 pathway plays a significant role in malignant transformation [36]. Li et al. demonstrated a crucial link between CCL18 derived from M2-like TAMs and Src/ERK1/2 signaling in breast cancer [37].

This study demonstrates that the addition of WCF in NSCLC cells inhibits $CD163^+$ TAM polarization and M2-like TAM-derived cytokine production in a co-culture system. WCF impedes NSCLC metastasis on TAM-induced EMT by antagonistically modulating CCL18. The anti-cancer effect of WCF is partially attributed to the regulation of M2 macrophages. Furthermore, the inhibition of invasive capability in A549 cells may involve Src/ERK1/2 activation in tumor cells. Notably, we established that WCF neutralized rCCL18 injection-induced metastasis of xenografts. Macrophages can accelerate their M2 polarization through autocrine CCL18, and CCL18 derived from tumor cells can recruit macrophages to the tumor site to induce M2 polarization. The binding of chemokines and their receptors triggers the activation and phosphorylation of Src/ERK1/2, and the phosphorylated ERK1/2 protein activates EMT-related transcription factor activity [38, 39]. However, metastasis is a multi-factorial process, necessitating further research to properly explore therapeutic approaches. Specifically, investigations are needed on the application of multiple therapeutic strategies, such as blocking the activity of CCL18 and other pro-tumor factors.

In our animal experiments, we employed a cell-derived xenograft mouse model to investigate whether WCF inhibits lung cancer metastasis by mitigating TAM-induced EMT in NSCLC cells. This model provides valuable biological tools for studying tumor progression from the establishment of lung tumors to the development of micro-metastases, closely mimicking the natural course of NSCLC in human patients [40]. Tumor implantation and longitudinal growth, localized almost exclusively in the lung, were evaluated using BLI [41]. Our study demonstrated that rCCL18 promoted tumor growth and metastasis *in vivo* compared to the control group, while WCF intervention mitigated these effects. These findings indicate that WCF counteracted the rCCL18-induced increase in xenograft growth and metastasis, aligning with our *in vitro* results. To further investigate the impact of WCF on M2 macrophages and lung cancer metastasis, additional animal experiments using immunocompetent mice should be conducted. This limitation represents an area for future research in our study.

The "formula" (like WCF) is the primary application mode of herbal medicine in TCM. It combines several herbs under the guidance of TCM theory. The complexity of effective components in TCM formulas presents a significant challenge for comprehensive research, which is the main limitation of this study. In our investigation, we characterized the chemical composition of WCF, identifying various ingredients such as ginsenoside, emodin, ferulic acid, and others [15]. Certain plants in WCF or their extracts, including ginsenoside Rb1 (Renshen), emodin (Dahuang), ferulic acid (Danggui), and aconitine (Fuzi), have been extensively studied and used clinically or preclinically [42-45]. While oral administra-

tion is the primary form of Chinese herbal medicine, the active ingredients are limited, and only those absorbed into the bloodstream can exert effects. Serum pharmacology offers a more scientific and effective method for *in vitro* experiments of TCM formulas compared to crude extracts. Our previous studies [46] qualitatively detected ginseng saponins Rb1, emodin, and aconitine in WCF-containing serum using high-performance liquid chromatogram (HPLC). Research has shown that emodin can induce M2 to M1 macrophage transformation and reverse the up-regulation of PCNA, TGF-β1, and p-Akt induced by M2 macrophages [47]. Aconitine-containing agents have been found to stimulate ROS production by TAMs and enhance the anti-tumor activity of dichloroacetate against Ehrlich carcinoma [12]. Recent studies have also demonstrated that ginsenoside Rb1 exhibits anti-proliferative effects on lung cancer cells [48] and enhances macrophage phagocytic capacity *via* activation of the p38/Akt pathway [49]. Additionally,

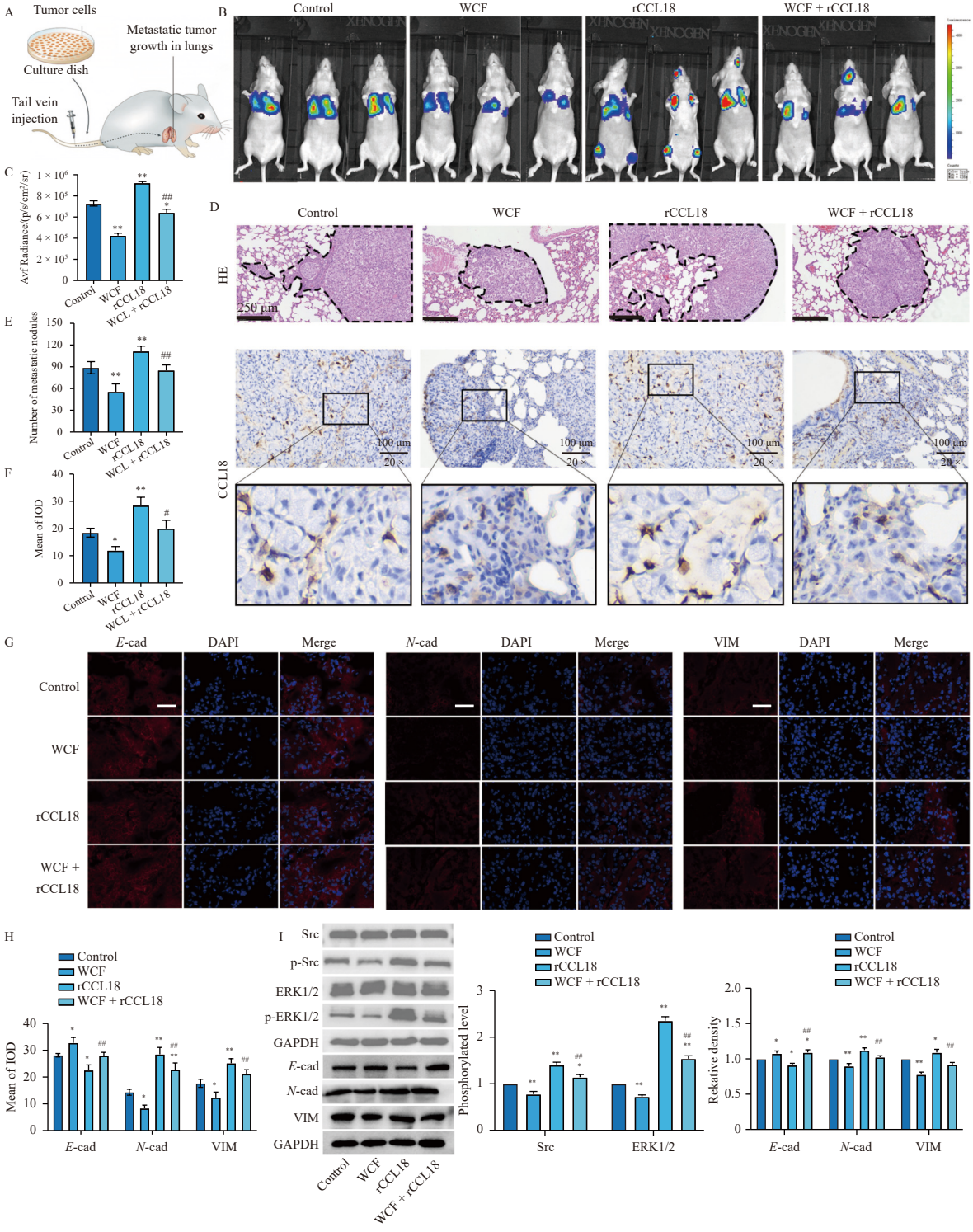

Fig. 5 WCF neutralized rCCL18 increased growth and metastasis of xenograft. (A) Schematic illustration of cell derived xenograft mouse model production. (B, C) Representative examples of ventral BLI views of tumor burden on days 35 from the four cohorts of mice are shown. (D) H&E staining and IHC staining for protein levels of CCL18. (E) statistical analysis for metastatic nodules in dissected lung specimen from mice (n = 5). (F) Statistical analysis of CCL18 protein level. (G, H) The expression of EMT markers were examined by immunofluorescence analysis (scale bars, 200 μm). (I) Western blotting analysis. Data are presented as mean ± SD from three independent experiments. $^{*}P < 0.05$, $^{**}P < 0.01$ *vs* control; $^{\#}P < 0.05$, $^{\#\#}P < 0.01$ *vs* rCCL18. *E*-cad, *E*-cadherin; *N*-cad, *N*-cadherin; VIM, Vimentin; rCCL18, recombinant CCL18.

ginsenosides Rg3-based liposomes loaded with paclitaxel have shown inhibition of IL-6/STAT3/p-STAT3 pathway activation, repolarizing protumor M2 macrophages to anti-tumor M1 phenotype in breast cancer [50]. These findings suggest that ginseng saponins Rb1, emodin, ginsenosides Rg3, and aconitine may be active ingredients of WCF. The aforementioned components of WCF show potential in regulating TAMs, providing a foundation for further research on the pharmacodynamic components of WCF. As the material basis of WCF, these components warrant further investigation, and their anti-cancer mechanisms require additional exploration.

5. Conclusion

In conclusion, WCF demonstrates inhibitory effects on Src/ERK1/2 signaling by antagonistically modulating CCL18, thereby regulating the interaction between TAMs and NSCLC cells (Fig. 6). WCF suppresses the upstream molecule TAM-derived CCL18, which is known to promote NSCLC cell proliferation and invasion. Additionally, WCF inhibits NSCLC metastasis by impacting TAM-induced EMT and reversing the polarization of M2-like TAMs. These findings suggest that WCF may serve as a potential therapeutic agent targeting M2-like TAMs for NSCLC treatment.

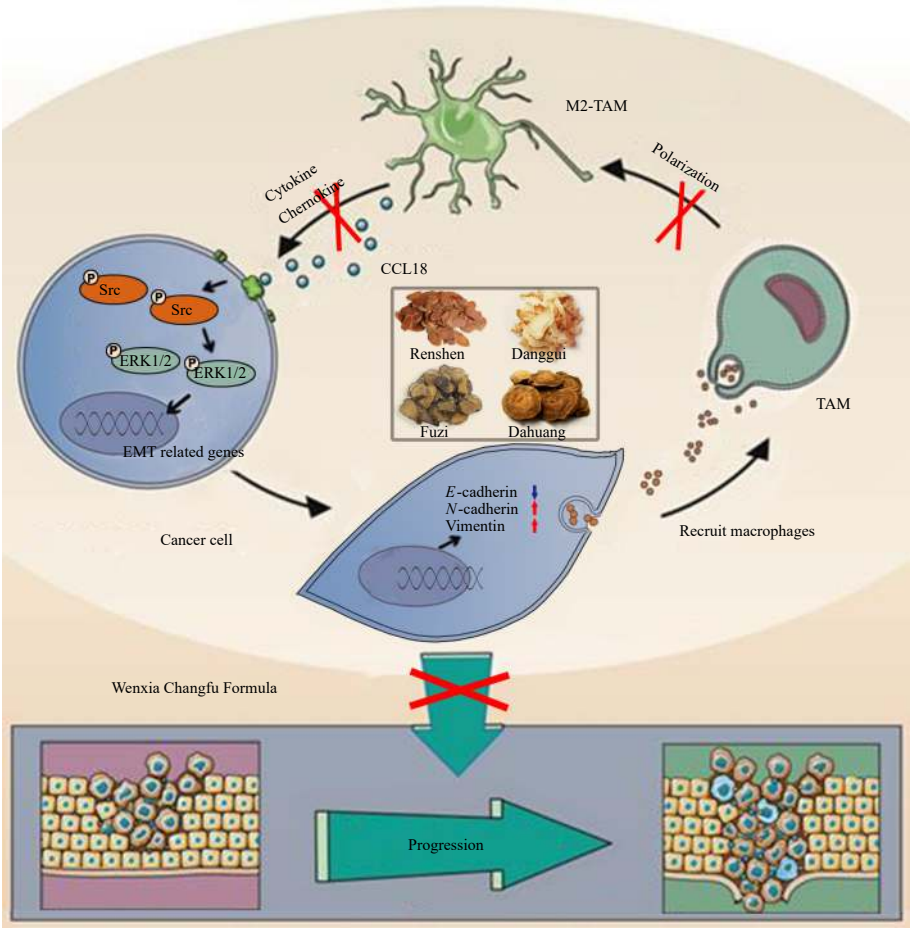

Fig. 6 The schematic illustration of anti-tumor effects of WCF. WCF suppresses the activation of Src and ERK in macrophages-activated NSCLC cells, resulting in the reduced production of CCL18. In addition, treatment with WCF reduces the M2 type polarization of macrophages induced by NSCLC cells.

Declarations

Ethics approval and consent to participate

The animal protocols were approved by the Animal Ethical and Welfare Committee of Zhejiang Chinese Medical University and conducted according to National Regulations in China (Ethical approval number: 20200506-11). All animal care and experimental procedures strictly adhered to the ARRIVE Guidelines.

Availability of data and materials

The data that support the findings of this study are available from the corresponding author upon reasonable request.

Funding

This study was supported by the National Natural Science Foundation of China (No. 82274406, 81774198), Zhejiang Provincial Natural Science Foundation of China (No. LZ24H270001) and the Postgraduate Scientific Research Fund of Zhejiang Chinese Medical University (No. 2022YKJ14).

Declaration of competing interest

These authors have no conflict of interest to declare.

References

1 Siegel RL, Giaquinto AN, Jemal A. Cancer statistics, 2024. *CA Cancer J Clin*. 2024;74(1):12-49. https://doi.org/10.3322/caac.21820.
2 Li C, Lei S, Ding L, et al. Global burden and trends of lung cancer incidence and mortality. *Chin Med J (Engl)*. 2023;136(13):1583-1590. https://doi.org/10.1097/CM9.0000000000002529.
3 Rasmussen RK, Etzerodt A. Therapeutic targeting of tumor-associated macrophages. *Adv Pharmacol*. 2021;91:185-211. https://doi.org/10.1016/bs.apha.2021.03.002.
4 Su P, Li O, Ke K, et al. Targeting tumor-associated macrophages: critical players in tumor progression and therapeutic strategies (Review). *Int J Oncol*. 2024;64(6):60. https://doi.org/10.3892/ijo.2024.5648.

5 Shefler I, Salamon P, Zitman-Gal T, et al. Tumor-derived extracellular vesicles induce CCL18 production by mast cells: a possible link to angiogenesis. *Cells*. 2022;11(3):353. https://doi.org/10.3390/cells11030353.
6 Huang X, Lai S, Qu F, et al. CCL18 promotes breast cancer progression by exosomal miR-760 activation of ARF6/Src/PI3K/Akt pathway. *Mol Ther Oncolytics*. 2022;25:1-15. https://doi.org/10.1016/j.omto.2022.03.004.
7 Caner A, Asik E, Ozpolat B. SRC signaling in cancer and tumor microenvironment. *Adv Exp Med Biol*. 2021;1270:57-71. https://doi.org/10.1007/978-3-030-47189-7_4.
8 Tan S, Tang H, Wang Y, et al. Tumor cell-derived exosomes regulate macrophage polarization: emerging directions in the study of tumor genesis and development. *Heliyon*. 2023;9(9):e19296. https://doi.org/10.1016/j.heliyon.2023.e19296.
9 Jin J, Yu G. Hypoxic lung cancer cell-derived exosomal miR-21 mediates macrophage M2 polarization and promotes cancer cell proliferation through targeting IRF1. *World J Surg Oncol*. 2022;20(1):241. https://doi.org/10.1186/s12957-022-02706-y.
10 Zhang Y, Wu Z, Yu H, et al. Chinese herbal medicine Wenxia Changfu Formula reverses cell adhesion-mediated drug resistance *via* the integrin *β*1-PI3K-AKT pathway in lung cancer. *J Cancer*. 2019;10(2):293-304. https://doi.org/10.7150/jca.25163.
11 Bi Q, Wang M, Zhao F, et al. *N*-Butanol fraction of Wenxia Formula extract inhibits the growth and invasion of non-small cell lung cancer by down-regulating Sp1-mediated MMP2 expression. *Front Pharmacol*. 2020;11:594744. https://doi.org/10.3389/fphar.2020.594744.
12 Pyaskovskaya ON, Boychuk IV, Fedorchuk AG, et al. Aconitine-containing agent enhances antitumor activity of dichloroacetate against Ehrlich carcinoma. *Exp Oncol*. 2015;37(3):192-196. https://doi.org/10.31768/2312-8852.2015.37(3):192-196.
13 Liu Q, Hodge J, Wang J, et al. Emodin reduces breast cancer lung metastasis by suppressing macrophage-induced breast cancer cell epithelial-mesenchymal transition and cancer stem cell formation. *Theranostics*. 2020;10(18):8365-8381. https://doi.org/10.7150/thno.45395.
14 Li H, Huang N, Zhu W, et al. Modulation the crosstalk between tumor-associated macrophages and non-small cell lung cancer to inhibit tumor migration and invasion by ginsenoside Rh2. *BMC Cancer*. 2018;18(1):579. https://doi.org/10.1186/s12885-018-4299-4.
15 Wang MR, Chen RJ, Zhao F, et al. Effect of Wenxia Changfu Formula combined with cisplatin reversing non-small cell lung cancer cell adhesion-mediated drug resistance. *Front Pharmacol*. 2020;11:500137. https://doi.org/10.3389/fphar.2020.500137.
16 Wang M, Bi QY, Zhang YN, et al. The anti-lung cancer effect of ethyl acetate extract from Wenxia Formula *in vivo via* the hedgehog-Gli1 signaling pathway mediated by cancer associated fibroblasts. *Arch Med Sci*. 2020;2020:106. https://doi.org/10.5114/aoms.2020.100106.
17 Chen W, Chen M, Hong L, et al. M2-like tumor-associated macrophage-secreted CCL2 facilitates gallbladder cancer stemness and metastasis. *Exp Hematol Oncol*. 2024;13(1):83. https://doi.org/10.1186/s40164-024-00550-2.
18 Rotolo A, Caputo VS, Holubova M, et al. Enhanced anti-lymphoma activity of CAR19-iNKT cells underpinned by dual CD19 and CD1d targeting. *Cancer Cell*. 2018;34(4):596-610. https://doi.org/10.1016/j.ccell.2018.08.017.
19 Wang CQ, Yi LW, Zhao L, et al. 177 saponins, including 11 new compounds in wild ginseng tentatively identified *via* HPLC-IT-TOF-MS$^{(n)}$, and differences among wild ginseng, ginseng under forest, and cultivated ginseng. *Molecules*. 2021;26(11):3371. https://doi.org/10.3390/molecules26113371.
20 He F, Wang CJ, Xie Y, et al. Simultaneous quantification of nine aconitum alkaloids in Aconiti Lateralis Radix Praeparata and related products using UHPLC-QQQ-MS/MS. *Sci Rep*. 2017;7(1):13023. https://doi.org/10.1038/s41598-017-13499-6.
21 Wang L, Huang S, Chen B, et al. Characterization of the anticoagulative constituents of Angelicae Sinensis Radix and their metabolites in rats by HPLC-DAD-ESI-IT-TOF-MS^n. *Planta Med*. 2016;82(4):362-370. https://doi.org/10.1055/s-0035-1558309.
22 Yan Y, Zhang Q, Feng F. HPLC-TOF-MS and HPLC-MS/MS combined with multivariate analysis for the characterization and discrimination of phenolic profiles in nonfumigated and sulfur-fumigated rhubarb. *J Sep Sci*. 2016;39(14):2667-2677. https://doi.org/10.1002/jssc.201501382.
23 Dallavalasa S, Beeraka NM, Basavaraju CG, et al. The role of tumor associated macrophages (TAMs) in cancer progression, chemoresistance, angiogenesis and metastasis: current status. *Curr Med Chem*. 2021;28(39):8203-8236. https://doi.org/10.2174/0929867328666210720143721.
24 Aehnlich P, Powell RM, Peeters MJW, et al. TAM receptor inhibition-implications for cancer and the immune system. *Cancers (Basel)*. 2021;13(6):1195. https://doi.org/10.3390/cancers13061195.
25 Yan S, Wan G. Tumor-associated macrophages in immunotherapy. *FEBS J*. 2021;288(21):6174-6186. https://doi.org/10.1111/febs.15726.
26 Huang H, Li J, Hu WJ, et al. The serum level of CC chemokine ligand 18 correlates with the prognosis of non-small cell lung cancer. *Int J Biol Markers*. 2019;34(2):156-162. https://doi.org/10.1177/1724600819829758.
27 Plönes T, Krohn A, Burger M, et al. Serum level of CC-chemokine ligand 18 is increased in patients with non-small-cell lung cancer and correlates with survival time in adenocarcinomas. *PLoS One*. 2012;7(7):e41746. https://doi.org/10.1371/journal.pone.0041746.
28 Kong S, Ding L, Fan C, et al. Global analysis of lysine acetylome reveals the potential role of CCL18 in non-small cell lung cancer. *Proteomics*. 2021;21(7-8):e2000144. https://doi.org/10.1002/pmic.202000144.
29 Zhang J, Hu Z, Horta CA, et al. Regulation of epithelial-mesenchymal transition by tumor microenvironmental signals and its implication in cancer therapeutics. *Semin Cancer Biol*. 2023;88:46-66. https://doi.org/10.1016/j.semcancer.2022.12.002.
30 Ding D, Zhang L, Liu X, et al. Chemokine CCL18 promotes phagocytosis through its receptor CCR8 rather than PITPNM3 in human microglial cells. *J Interferon Cytokine Res*. 2022;42(1):19-28. https://doi.org/10.1089/jir.2021.0123.
31 Korbecki J, Olbromski M, Dzięgiel P. CCL18 in the progression of cancer. *Int J Mol Sci*. 2020;21(21):7955. https://doi.org/10.3390/ijms21217955.
32 Chen RH, Xiao ZW, Yan XQ, et al. Tumor cell-secreted ISG15 promotes tumor cell migration and immune suppression by inducing the macrophage M2-like phenotype. *Front Immunol*. 2020;11:594775. https://doi.org/10.3389/fimmu.2020.594775.
33 Poh AR, Ernst M. Functional roles of SRC signaling in pancreatic cancer: recent insights provide novel therapeutic opportunities. *Oncogene*. 2023;42(22):1786-1801. https://doi.org/10.1038/s41388-023-02701-x.
34 Fang R, Chen X, Zhang S, et al. EGFR/SRC/ERK-stabilized YTHDF2 promotes cholesterol dysregulation and invasive growth of glioblastoma. *Nat Commun*. 2021;12(1):177. https://doi.org/10.1038/s41467-020-20379-7.
35 Aravind A, Palollathil A, Rex DAB, et al. A multi-cellular molecular signaling and functional network map of C-C motif chemokine ligand 18 (CCL18): a chemokine with immunosuppressive and pro-tumor functions. *J Cell Commun Signal*. 2022;16(2):293-300. https://doi.org/10.1007/s12079-021-00633-3.
36 Khan T, Kryza T, Lyons NJ, et al. The CDCP1 signaling hub: a target for cancer detection and therapeutic intervention. *Cancer Res*. 2021;81(9):2259-2269. https://doi.org/10.1158/0008-5472.CAN-20-2978.
37 Li HY, Cui XY, Wu W, et al. Pyk2 and Src mediate signaling to CCL18-induced breast cancer metastasis. *J Cell Biochem*. 2014;115(3):596-603. https://doi.org/10.1002/jcb.24697.
38 Schmid S, Le UT, Haager B, et al. Local concentrations of CC-chemokine-ligand 18 correlate with tumor size in non-small cell lung cancer and are elevated in lymph node-positive disease. *Anticancer Res*. 2016;36(9):4667-4671. https://doi.org/10.21873/anticanres.11018.
39 Schmidt-Wolf R, Zissel G. Interaction between CCL18 and GPR30 differs from the interaction between estradiol and GPR30. *Anticancer Res*. 2020;40(6):3097-3108. https://doi.org/10.21873/anticanres.14291.
40 Jarry U, Bostoën M, Pineau R, et al. Orthotopic model of lung cancer: isolation of bone micro-metastases after tumor escape from osimertinib treatment. *BMC Cancer*. 2021;21(1):530. https://doi.org/10.1186/s12885-021-08205-9.
41 Mordant P, Loriot Y, Lahon B, et al. Bioluminescent orthotopic mouse models of human localized non-small cell lung cancer: feasibility and identification of circulating tumour cells. *PLoS One*. 2011;6(10):e26073. https://doi.org/10.1371/journal.pone.0026073.
42 Lu S, Zhang Y, Li H, et al. Ginsenoside Rb1 can ameliorate the key inflammatory cytokines TNF-α and IL-6 in a cancer cachexia mouse model. *BMC Complement Med Ther*. 2020;20(1):11. https://doi.org/10.1186/s12906-019-2797-9.
43 Wu JJ, Zhu YF, Guo ZZ, et al. Aconitum alkaloids, the major components of Aconitum species, affect expression of multidrug resistance-associated protein 2 and breast cancer resistance protein by activating the Nrf2-mediated signalling pathway. *Phytomedicine*. 2018;44:87-97. https://doi.org/10.1016/j.phymed.2017.12.007.
44 Zheng Y, You X, Chen L, et al. Biotherapeutic nanoparticles of poly(ferulic acid) delivering doxorubicin for cancer therapy. *J Biomed Nanotechnol*. 2019;15(8):1734-1743. https://doi.org/10.1166/jbn.2019.2798.
45 Zou G, Zhang X, Wang L, et al. Herb-sourced emodin inhibits angiogenesis of breast cancer by targeting VEGFA transcription. *Theranostics*. 2020;10(15):6839-6853. https://doi.org/10.7150/thno.43622.
46 Ji XM, Ouyang B, Liu H, et al. *In vitro* and *in vivo* inhibitory effect of the combination of Wenxia Changfu Formula with cisplatin in non-small cell lung cancer. *Chin J Integr Med*. 2011;17(12):908-916. https://doi.org/10.1007/s11655-011-0934-5.
47 Yin J, Zhao X, Chen X, et al. Emodin suppresses hepatocellular carcinoma growth by regulating macrophage polarization *via* microRNA-26a/transforming growth factor beta 1/protein kinase B. *Bioengineered*. 2022;13(4):9548-9563. https://doi.org/10.1080/21655979.2022.2061295.
48 Ding L, Qi H, Wang Y, et al. Recent advances in ginsenosides against respiratory diseases: therapeutic targets and potential mechanisms. *Biomed Pharmacother*. 2023;158:114096. https://doi.org/10.1016/j.biopha.2022.114096.
49 Xin C, Quan H, Kim JM, et al. Ginsenoside Rb1 increases macrophage phagocytosis through p38 mitogen-activated protein kinase/Akt pathway. *J Ginseng Res*. 2019;43(3):394-401. https://doi.org/10.1016/j.jgr.2018.05.003.
50 Zhu Y, Wang A, Zhang S, et al. Paclitaxel-loaded ginsenoside Rg3 liposomes for drug-resistant cancer therapy by dual targeting of the tumor microenvironment and cancer cells. *J Adv Res*. 2023;49:159-173. https://doi.org/10.1016/j.jare.2022.09.007.